Quantum Electronics **45** (1) 26–34 (2015)

NONLINEAR OPTICAL PHENOMENA

PACS numbers: 42.55.Wd; 42.60.Fc; 42.81.Dp
DOI: 10.1070/QE2015v045n01ABEH015558

Generation of bound states of pulses in a soliton laser with complex relaxation of a saturable absorber

I.O. Zolotovskii, D.A. Korobko, R.V. Gumenyuk, O.G. Okhotnikov

Abstract. **A numerical model of a soliton fibre laser with a semiconductor saturable absorber mirror (SESAM), characterised by the complex dynamics of absorption relaxation, is considered. It is shown that stationary bound states of pulses can be formed in this laser as a result of their interaction via the dispersion-wave field. The stability of stationary bound states of several pulses is analysed. It is shown that an increase in the number of pulses in a stationary bound state leads eventually to its decay and formation of a random bunch. It is found that the bunch stability is caused by the manifestation of nonlinear self-phase modulation, which attracts pulses to the bunch centre. The simulation results are in qualitative agreement with experimental data.**

Keywords: *soliton fibre laser, semiconductor saturable absorber mirror, bound states of pulses.*

1. Introduction

It is known that passively mode-locked fibre lasers with an anomalous-dispersion cavity are generators of soliton-like pulses, the duration and energy of which are in unambiguous correspondence. The pulse duration is basically determined by the cavity parameters (i.e., the cavity length, dispersion and characteristics of a saturable absorber) [1]. An insignificant increase in pumping only slightly affects the pulse parameters, changing mainly the non-soliton component of radiation. A more pronounced increase in pumping leads to a successive increase in the number of pulses in the cavity [2–5]. As a result, the cavity may contain a large number of pulses and the time intervals (which can be referred to as distances) between pulses change constantly, which is mainly related to the interaction between pulses and the non-soliton component of radiation [6]. The change in the interpulse distance can also be affected by gain saturation [3], electrostriction and acoustic effects [7–9].

One of the key elements of a laser source of ultrashort pulses is a saturable absorber. The most popular saturable absorbers are based on either carbon nanotubes [10] or semiconductor saturable absorber mirrors (SESAMs) [11, 12]. Note that a semiconductor saturable absorber may exhibit both fast (with characteristic times $\tau < 1$ ps) and slow ($\tau \sim 1$ ps) dynamics of absorption recovery [1]. This is related to resonant or nonresonant absorption in the bulk of a semiconductor or in the structure of quantum dots and wires. Resonant excitation and absorption of charge carriers are related to the slow absorption component. The near-resonance effects at the band edges, intraband scattering of carriers and thermalisation processes are characterised by short (subpicosecond) recovery times [11]. Various designs of saturable absorbers based on semiconductor structures are used in lasers; they differ in both the characteristic recovery times of each component and the contribution to absorption. Thus, one can select two groups of saturable absorbers with predominantly slow or fast responses. It is noteworthy that mode locking and generation of subpicosecond pulses in a soliton fibre laser can be implemented using both fast and slow (with a relaxation time of several tens of picoseconds) saturable absorbers; however, a fast saturable absorber is much more suitable to provide the pulse stability and suppress the spurious non-soliton component [1]. Thus, when developing fibre soliton lasers, the technologies aimed at shortening the saturable-absorber response time (based on low-temperature and metamorphic growth of semiconductor structures, ion irradiation, etc.) become of key importance [12–14].

In this study we consider a model of a soliton laser based on a semiconductor saturable absorber mirror with a complex absorption recovery dynamics (fast and slow relaxation); the slow-component relaxation time is sufficiently long ($\tau > 100$ ps). Our experiments show that a SESAM, which possesses only slow response with this relaxation time, cannot initiate mode locking and may cause only instable operation of a Q-switched laser [15]. At the same time, the absorbers of SESAM type have a number of interesting properties. First, they are characterised by more rapid switching on of mode locking [16]. The second (and especially important) feature are the interesting patterns of complex pulse dynamics, which is observed in the cavity of soliton lasers with a saturable absorber of this type. The aforementioned dynamics, at which pulses are independently located in the cavity and the distances between them constantly change, is typical of lasers based on standard 'fast' saturable absorbers. The lasers based on a SESAM with complex relaxation may demonstrate a qualitatively different joint dynamics of pulses: their mutual attraction with formation of stable bound states of solitons with equal and constant distances between them (up to 100 pulse durations) or grouping pulses into a close random bunch with small and continuously

I.O. Zolotovskii, D.A. Korobko Ulyanovsk State University, ul. L'va Tolstogo 42, 432700 Ul'yanovsk, Russia;
e-mail: korobkotam@rambler.ru;
R.V. Gumenyuk Optoelectronics Research Centre, Tampere University of Technology, Korkeakoulunkatu 3, 33101, Tampere, Finland;
O.G. Okhotnikov Ulyanovsk State University, ul. L'va Tolstogo 42, 432700 Ul'yanovsk, Russia; Optoelectronics Research Centre, Tampere University of Technology, Korkeakoulunkatu 3, 33101, Tampere, Finland

Received 14 May 2014; revision received 16 June 2014
Kvantovaya Elektronika **45** (1) 26–34 (2015)
Translated by Yu.P. Sin'kov

changing interpulse distances. The behaviour of these pulse groups is determined by the cavity parameters [15–18].

The purpose of our study si to analyse the joint dynamics of several pulses in the cavity of aforementioned lasers, determine the nature of interaction between pulses and specify the influence of cavity parameters on the characteristics of soliton groups. Determination of the conditions for generating stationary bound states with a constant interpulse distance and revealing of negative factors leading to the formation of random soliton bunches may also have applied importance (potential use of laser sources of bound solitons as master oscillators, in metrological problems, etc.).

To solve the above-stated problem, we simulated a fibre laser with a 'two-time' saturable absorber SESAM having different cavity parameters, under different pump levels and initial conditions.

2. Model

Let us consider the following model of a fibre laser (Fig. 1). Propagation of radiation in active and passive fibre elements is described by the Ginzburg–Landau equation and nonlinear Schrödinger equation (NLSE), respectively:

$$\frac{\partial A}{\partial z} + \mathrm{i}\frac{\beta_{2\mathrm{a}} - \mathrm{i}\beta_{2\mathrm{f}}}{2}\frac{\partial^2 A}{\partial t^2} - \mathrm{i}\gamma_{\mathrm{a}}|A|^2 A = (g - l_{\mathrm{a}})A, \tag{1a}$$

$$\frac{\partial A}{\partial z} + \mathrm{i}\frac{\beta_{2\mathrm{p}}}{2}\frac{\partial^2 A}{\partial t^2} - \mathrm{i}\gamma_{\mathrm{p}}|A|^2 A = -l_{\mathrm{p}}A. \tag{1b}$$

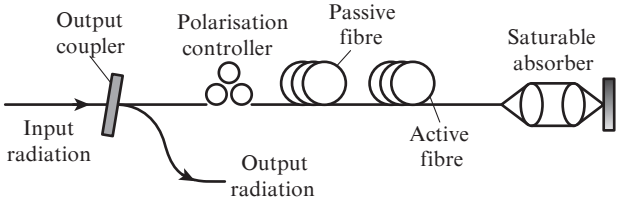

Figure 1. Schematic diagram of the laser used in simulation.

Here, $A(z, t)$ is a slowly varying field amplitude; z is the coordinate along the cavity; t is time in the related coordinate system; $\beta_{2\mathrm{a}}$, $\beta_{2\mathrm{p}}$, γ_{a} and γ_{p} are the group-velocity dispersions and Kerr nonlinearity coefficients for the active and passive fibres, respectively; and l_{a} and l_{p} are the loss factors in the active and passive fibres, respectively. Spectral gain filtering is taken into account through coefficient $\beta_{2\mathrm{f}} = g/\Omega_{\mathrm{f}}^2$, i.e., a parabolic approximation of the gain line with a half-width Ω_{f} is used. Furthermore, we will be interested in only the soliton regime, i.e., the cavity is assumed to have a significant anomalous dispersion $2\beta_{2\mathrm{a}}L_{\mathrm{a}} + 2\beta_{2\mathrm{p}}L_{\mathrm{p}} < 0$, where L_{a} and L_{p} are the lengths of active and passive fibres, respectively. The dynamics of the saturable gain g is determined by the standard equation

$$\frac{\mathrm{d}g}{\mathrm{d}\tau} = \frac{g_0 - g}{\tau_g} - \frac{g|A(z,\tau)|^2}{\tau_g P_g}, \tag{2}$$

where g_0 is the small-signal gain, τ_{g} is the relaxation time and P_{g} is the active-medium saturation power. In the case under consideration, the active-medium relaxation time is sufficiently long in comparison with the individual pulse duration and cavity round-trip time T_{r}; therefore, the saturable gain can be replaced with the cavity-averaged value

$$g(z,\tau) = g(z) = g_0\left[1 + \frac{\int_0^{T_{\mathrm{r}}}|A(z,\tau)|^2\,\mathrm{d}\tau}{P_g T_{\mathrm{r}}}\right]^{-1}. \tag{3}$$

In addition, the wave field in the cavity is affected by discrete elements: saturable absorber, output coupler and polariser. This influence can be described by the transfer function

$$A_{\mathrm{out}} = JA_{\mathrm{in}}.$$

For example, the output coupler with a coupling ratio R can be presented as a discrete element with a transfer coefficient $A_{\mathrm{out}} = \sqrt{1-R}\,A_{\mathrm{in}}$.

In this model we neglect the vector nature of solitons in a fibre laser, and the operation of polarisation filters is qualitatively described using the effective model for the transfer function [19, 20]:

$$J = \sin^2\vartheta\sin^2\varphi + \cos^2\vartheta\cos^2\varphi + \frac{1}{2}\sin(2\vartheta)\sin(2\varphi)\cos(\varphi_{\mathrm{fib}} + \varphi_{\mathrm{pol}}). \tag{4}$$

Here, ϑ and φ are, respectively, the polariser and analyser orientation angles; φ_{fib} is the phase accumulated during transmission through the fibre; and φ_{pol} is the phase jump caused by passage through the polariser.

The saturable absorber used in our model has two characteristic relaxation times, which correspond to the so-called fast and slow SESAM responses. The large difference in the relaxation times ($\tau_{\mathrm{slow}} \gg \tau_{\mathrm{fast}}$) and the smallness of absorption modulations ($\alpha_{\mathrm{fast}}, \alpha_{\mathrm{slow}} \ll 1$) suggest that the field interacts with the saturable absorber independently for each field component (this was confirmed experimentally [16]):

$$A_{\mathrm{out}} = [1 - \alpha_{\mathrm{slow}}(\tau)][1 - \alpha_{\mathrm{fast}}(\tau)]A_{\mathrm{in}}.$$

The dynamics of the absorption coefficient components $\alpha_{\mathrm{slow}}(\tau)$ and $\alpha_{\mathrm{fast}}(\tau)$ is described by equations of the same type:

$$\frac{\mathrm{d}\alpha_{\mathrm{slow}}}{\mathrm{d}\tau} = \frac{\alpha_{0\mathrm{slow}} - \alpha_{\mathrm{slow}}}{\tau_{\mathrm{slow}}} - \frac{\alpha_{\mathrm{slow}}|A(z',\tau)|^2}{E_{\mathrm{satslow}}}, \tag{5a}$$

$$\frac{\mathrm{d}\alpha_{\mathrm{fast}}}{\mathrm{d}\tau} = \frac{\alpha_{0\mathrm{fast}} - \alpha_{\mathrm{fast}}}{\tau_{\mathrm{fast}}} - \frac{\alpha_{\mathrm{fast}}|A(z',\tau)|^2}{E_{\mathrm{satfast}}}, \tag{5b}$$

where α_0 is the modulation depth; E_{satfast} and E_{satslow} are the saturation energies; and τ_{fast} and τ_{slow} are the relaxation times of the fast and slow absorbers, respectively. The first term on the right-hand side describes the absorber relaxation and the second term describes the saturable absorption. Since the fast-response relaxation time τ_{fast} is much shorter than the pulse duration, it can be simulated within the instantaneous response approximation:

$$\alpha_{\mathrm{fast}}(\tau) = \alpha_{0\mathrm{fast}}\left[1 + \frac{|A(\tau)|^2}{P_{\mathrm{satfast}}}\right]^{-1}. \tag{6}$$

3. Simulation of pulse bound states

The parameters used in the simulation were taken to be typical of Er-doped fibre lasers:

$\alpha_{0\,\mathrm{fast}} = \alpha_{0\,\mathrm{slow}}$	0.05
$P_{\mathrm{sat\,fast}}$/W	20
$E_{\mathrm{sat\,slow}}$/pJ	15
τ_{slow}/ps	200
$\gamma_a = \gamma_p/\mathrm{W}^{-1}\,\mathrm{m}^{-1}$	0.003
$l_a = l_p/\mathrm{m}^{-1}$	0.01
$\beta_{2a}/\mathrm{ps}^2\,\mathrm{m}^{-1}$	50
$\beta_{2p}/\mathrm{ps}^2\,\mathrm{m}^{-1}$	–16
L_a/m	0.6
L_p/m	6
g_0/m^{-1}	0.6
Ω_f/s^{-1}	6.7×10^{12}
φ_{pol}	$\pi/2$
φ	$\pi/25$
ϑ	$\pi/12$

At the aforementioned fibre dispersion values, the net cavity dispersion β_{net} is -0.132 ps^2.

Under the initial conditions imposed on the input radiation in the form of white noise and active-medium saturation energy $E_g = 30$ pJ, an individual pulse is generated. At the output point the pulse envelope is close to $|A(t)|^2 = P_0\mathrm{sech}^2(t/\tau_0)$; its parameters are in the vicinity of $P_0 \approx 68$ W and $\tau_0 = 0.28$ ps, values corresponding to an average pulse energy of about 39 pJ. Along with the pulse, the cavity contains also the so-called non-soliton component, whose origin is related to the perturbation of the pulse shape during amplification and transmission through individual discrete elements. To specify terminology, we will refer below to this component as dispersion waves (or oscillating tails of pulses).

Due to the presence of the slow component in a SESAM and the corresponding low absorption behind a pulse, the dispersion waves generated in this region have a higher intensity. Periodic scattering of pulse energy in the field of high-power dispersion waves leads to discrepancy between the period of variation in the pulse parameters and T_r. Calculations show that in the stationary single-pulse regime, a laser generates a pulse with characteristics changing with a period $\sim 3T_r$. The generated non-soliton field also evolves in the cavity under the action of discrete elements and dispersion effects. In total, this leads to small periodic changes in energy and peak pulse power with a period on the order of several tens of T_r (see Figs 5a and 5c). The existence of these oscillations is closely related to the nonlinear dynamics of dissipative solitons [21, 22].

To analyse the formation of a coupled state, we simulated this laser system with initial conditions in the form of two sech^2 pulses with durations of 0.28 ps at different distances between them; to implement generation of two pulses, the active-medium saturation energy E_g was increased to 60 pJ. It was shown that, for an initial interpulse distance of 8–15 ps and simulation of up to 2×10^4 cavity round trips, the two pulses form a bound state, in which they move jointly through the cavity with equal velocities, being spaced by a constant distance. The simulation results for an initial interpulse distance of 12 ps are shown in Figs 2–5.

The joint evolution of a pair of pulses is accompanied by their interaction via long oscillating tails. This interaction can be described using a conditional analogy with the interaction of two wave sources (floats) in a one-dimensional reservoir of linear waves (Fig. 2). The first pulse is located in the region of higher absorption of the slow component and has a lower peak power, while the second pulse is in the low-absorption region, has a high peak power, and emits more intense dispersion waves. The dispersion-wave powers are much lower than the pulse powers; they can be considered as linear, because the influence of nonlinearity in the interpulse region is negligible.

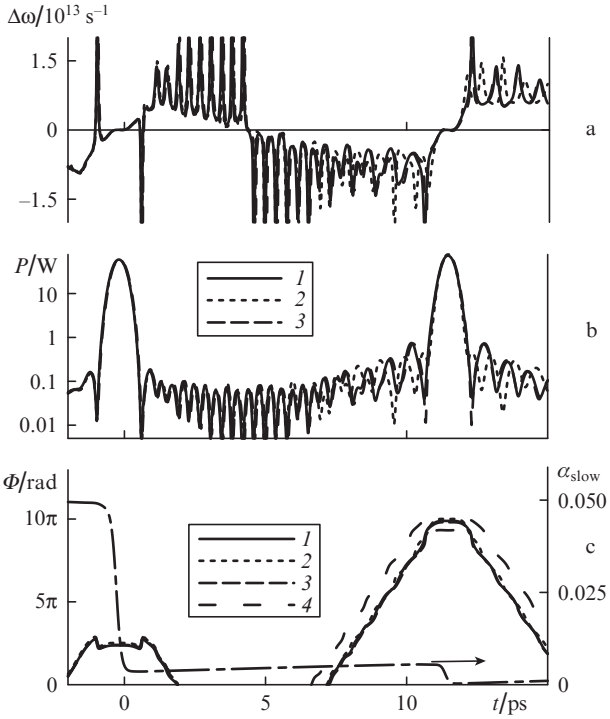

Figure 2. (a) Instantaneous frequency, (b) envelopes of pulses in a pair and (c) phases of pulses and the absorption level of the SESAM's slow component α_{slow}; (*1*) pulse parameters after 2000 cavity round trips; curves (*2*), (*3*) and (*4*) differ from (*1*) by 11, 33, and 3 cavity round trips, respectively.

As in the case of a single pulse, one can select some characteristic evolution periods for the pair of pulses. The short period ($3T_r$) is related to the evolution of the second, higher-power pulse in the cavity, while the second period ($11T_r$) is related to the periodic change in the dispersion-wave field. This assignment is illustrated in Fig. 2c, which shows the phase difference between pulses. It is determined by two contributions: a linear part, proportional to time and related to dispersion waves, and a nonlinear part, which depends on the peak pulse powers. Note that the phases corresponding to equal peak pulse powers [curves (*1*) and (*4*) in Fig. 2c] and having identical nonlinear contributions may nevertheless significantly differ. Thus, we can suggest that the phase difference is mainly determined by the linear part, related to long oscillating pulse tails. This suggestion is confirmed by the almost complete coincidence of curves (*1*) and (*2*), which differ only in the period of change in the dispersion-wave field (11 cavity round trips). Another confirmation is the spectra of states (*1*) and (*2*) (Fig. 3a). The spectrum of a pair of pulses has a characteristic lobate structure. The envelopes of interference spectra coincide with the individual-pulse spectrum; the frequency of the most intense dispersion waves can be estimated by the Kelley peak frequency $\Delta\omega_s$.

The spectrum acquires a lobate structure because of the interference between the spectra of two pulses, which are shifted with respect to each other by Δ; note that the lobe size is inversely proportional to the distance Δ between the pulse peaks. With a change in the phase difference between the pulses, the characteristic lobe size is retained, but the entire

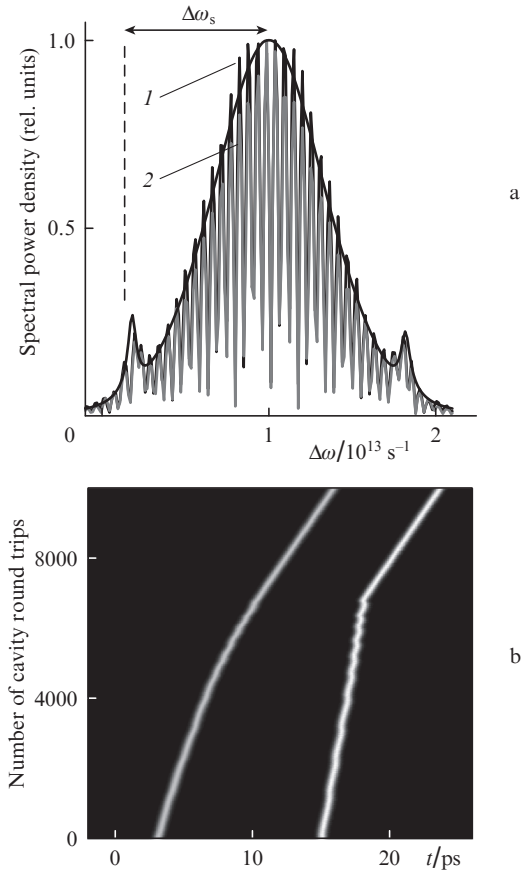

Figure 3. Spectra of states (*1*) and (*2*) from Fig. 2: (a) the envelope (single-pulse spectrum) and (b) the trajectory of a pair of pulses during the formation of a bound state.

structure of the spectrum is shifted. The identical structure of the spectra of states (*1*) and (*2*) in Fig. 3a confirms that these states have close phase characteristics. Small differences are related to the change in the second-pulse peak power. Recall that this value changes for a time of $3T_r$. A comparison of the pulse parameters (instantaneous frequency, amplitude and phase) differing by the common multiple evolution period $33T_r$ shows their almost complete coincidence (Fig. 2).

Nevertheless, the periodic repetitions of the characteristics of pulses and the dispersion field formed by these pulses are not absolutely identical. The interaction between pulses and dispersion-wave field leads to small fluctuations in the pulse positions. When observing interaction for a rather long time (on the order of 10^4 cavity round trips), one can note a change in the distance between pulses and formation of their bound state, in which pulses move with equal velocities (Fig. 3b). Our observations revealed that the oscillating tails of pulses merge into a general self-consistent field, and the bound state of pulses is formed as a result of their drift in this field. To clarify this issue, we will consider the interaction of pulses with the dispersion-wave field in more detail.

First, we will select the forces exerted by dispersion waves on the pulse producing them. Since the net cavity dispersion is anomalous, the frequency shift at the trailing edge of the pulse with respect to the carrier is positive, while the shift at the leading edge is negative (Fig. 2a). The evolution of dispersion-wave field u_d in fibre elements is linear; it is described by the following equations (the absorption and spectral filtering are disregarded):

$$\frac{\partial u_d}{\partial z} = -i\frac{\beta_{2p}}{2}\frac{\partial^2 u_d}{\partial t^2},$$

$$\frac{\partial u_d}{\partial z} = -i\frac{\beta_{2a}}{2}\frac{\partial^2 u_d}{\partial t^2} + g u_d.$$

A simple analysis of these equations shows that the function of the field amplitude u_d is proportional to the factor $\exp(i\omega[\beta_2\omega z/2 - t])$, which determines the dispersion flow direction. In the anomalous-dispersion region ($\beta_2 < 0$), dispersion waves move toward the pulse (wave source), whereas in the normal-dispersion region ($\beta_2 > 0$), they move away from the pulse. In addition, the dispersion field is affected by the saturable absorber. Due to the saturation of the slow component, the dispersion-wave intensity behind the pulse exceeds the intensity before it; this circumstance determines the pulse drift velocity in the dispersion-wave field.

Having analysed the saturation equation for the slow component (5b), with neglected absorption recovery for a time on the order of pulse duration, we find that the difference in the linear-wave absorption before and behind the pulse, $\Delta\alpha_{slow}$, is determined by the pulse energy E_p and the absorption before the pulse, $\alpha_{slow}(t_p)$:

$$\Delta\alpha_{slow} = \alpha_{slow}(t_p)\exp\left(-\frac{E_p}{E_{sat\,slow}}\right), \quad (7)$$

where t_p is the time coordinate directly before the pulse. On the assumption that the pulse energies have close values and the slow component in the vicinity of the second pulse is in a much more saturated state $\alpha_{slow}(t_2) < \alpha_{slow}(t_1)$, we obtain the condition $\Delta\alpha_{slow1} > \Delta\alpha_{slow2}$, which indicates that the difference in the dispersion-wave intensities near the second pulse is much smaller. Therefore, before the formation of a bound state, the velocity of the second-pulse drift (caused by the interaction with the dispersion waves produced by this pulse) is lower than the corresponding velocity of the first pulse.

Hence, one can conclude the following: pulses should repulse in a cavity having no normal-dispersion regions. Indeed, in this case, each pulse is constantly affected by a lateral force directed forward (toward less intense dispersion waves). The distance between the pulses will increase, because the first-pulse drift velocity greatly exceeds that of the second pulse. This process is presented in Fig. 4. Here, all parameters of the system are the same as in the case of formation of a

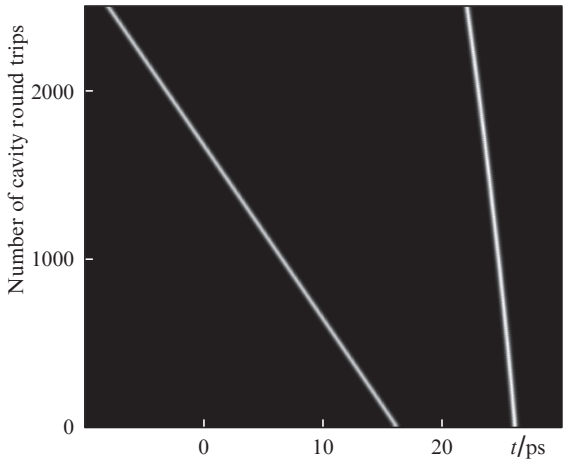

Figure 4. Trajectories of pulses in a pair at $\beta_{2a} = \beta_{2b} = -10$ ps^2 km^{-1}.

bound state; the only difference is that exactly the same net cavity dispersion is obtained for an active fibre with anomalous dispersion. In the absence of other pulses in the cavity, the walk-off of pulses occurs while $\Delta\alpha_{\text{slow1}} \approx \Delta\alpha_{\text{slow2}}$; this inequality is satisfied when $t_2 - t_1 > \tau_{\text{slow}}$. In this case, the characteristics of each pulse are asymptotically close to those of a single pulse in the cavity.

If there are normal-dispersion regions ($\beta_{2a} > 0$), the interaction of a pulse with the dispersion waves produced by it allows pulses to come closer (compare Figs 3b and 4). This process is shown in more detail in Fig. 5. Here, it is of importance that, beginning with a certain instant, each pulse is significantly affected by the dispersion waves produced by the second pulse of the pair. Initially, the dispersion waves from different pulses have different phases, and the neighbouring-pulse effect leads to only small fluctuations. The fluctuations increasing the distance between pulses (i.e., opposite to the tendency of pulses to approach) are suppressed. The fluctuations making pulses approach increase with decreasing interpulse distance, because the amplitude of interacting dispersion waves increases. This results in pulse approach with a constant acceleration (Figs 5b, 5d).

It can also be seen in Fig. 5 that the change in the distance between pulses has a characteristic step form. In contrast to the continuous repulsion in Fig. 4, which is related to the interaction between a pulse and a dispersion field induced by this pulse, the approaching pulse is affected by the counter-propagating dispersion-field source. Each step corresponds to a quasi-stationary bound state of pulses, when there are an integer number of dispersion-wave periods between them [23]. The interaction of a pulse with an intrinsic dispersion field shifts pulses to quasi-stationary states of a lower level, which corresponds to their further approach. In sum, the interference of pulse dispersion fields leads to the formation of a general self-consistent dispersion-wave field; the pulses form a stable bound state by interacting via this field.

The distance between pulses in the bound state is determined in many respects by the parameters of the slow component of a saturable absorber. Indeed, the difference in the dispersion field intensities before and behind each pulse should be such as to make equal the drift velocities of the pulses interacting with this field. A more careful analysis is planned to perform in order to clear up the relationship between the parameters of a SESAM's slow component, which specifies the differences in the dispersion-field intensities before and behind the pulses and the bound-state parameters.

The formation of a bound state is accompanied by an increase in the amplitude of peak power oscillations and

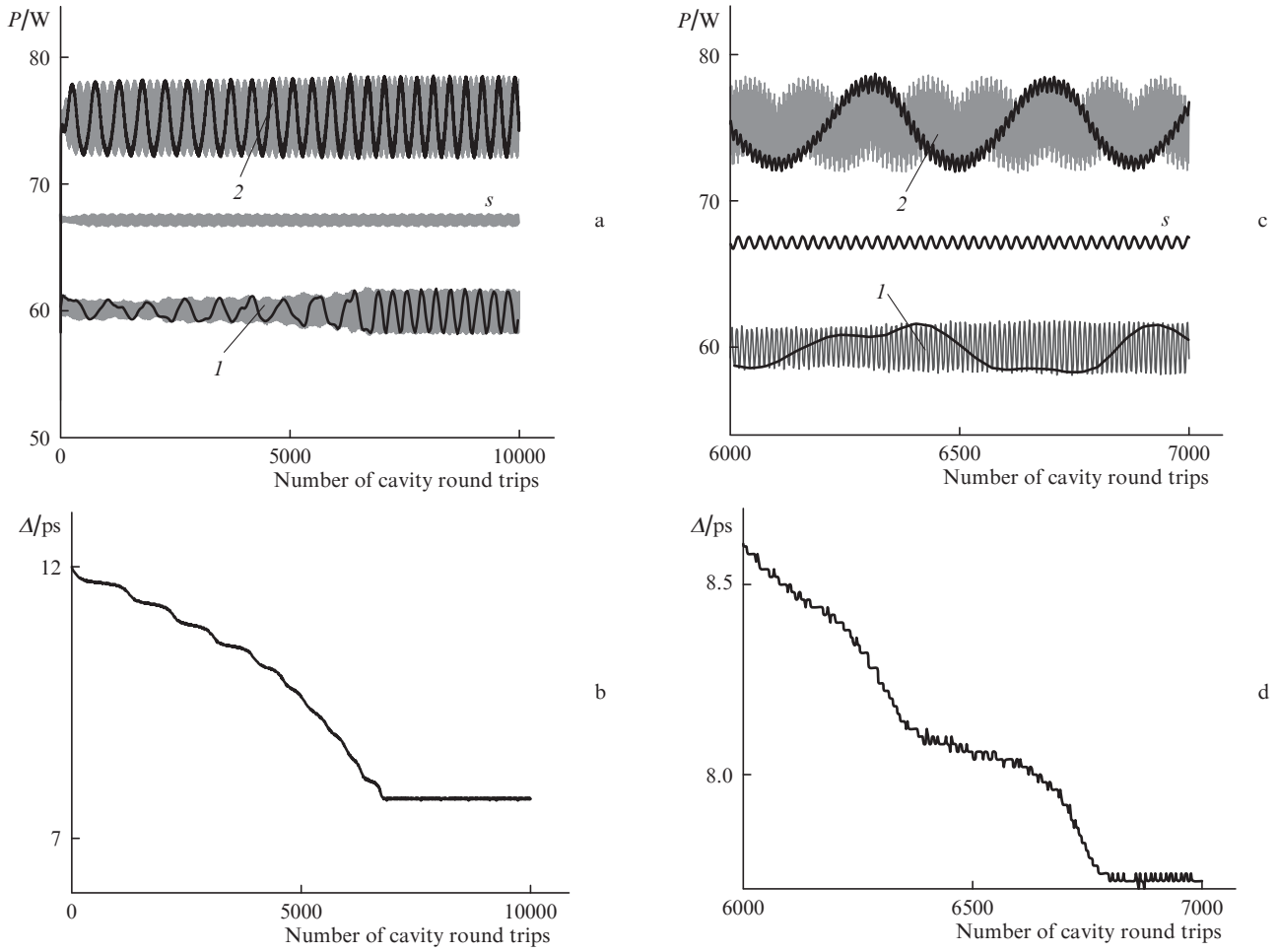

Figure 5. (a, c) Evolution of the peak powers of the (*1*) first and (*2*) second pulses during the formation of a bound state (the background is the values after each cavity round trip; (*1*) peak power after each 33rd cavity round trip by the first pulse, (*2*) peak power after each third cavity round trip by the second pulse, and *s* is the peak power of a single pulse; the values are taken after each third cavity round trip) and (b, d) the change in the distance between pulses.

matching of long periods of these oscillations (Figs 5a, 5c). This pattern is typical of the formation of a stable energy exchange between pulses. In the thus formed bound state, counterpropagating pulses exchange energy through long oscillating tails. Since the interfering tails are in phase, there is no energy loss. The amplitude of peak power oscillations increases because of partial transfer of pulse energy to the general field; i.e., due to the formation of binding energy.

The distance between pulses in the thus formed state of bound solitons exceeds 25 their durations, i.e., this state belongs to loosely bound ones. A periodic transfer of some part of pulse energy to the dispersion-wave field causes small fluctuations of the interpulse distance, which can be observed in Fig. 5d. These fluctuations correspond to transitions between two closely located points of the system equilibrium: the point of constant pulse (equilibrium of lateral forces) and the point of stationary energy [24].

To complete this section, it is important to note that the simulation result predicting impossibility of the bound-soliton-state formation in a laser with a two-time SESAM in the absence of normal-dispersion regions in the cavity was confirmed experimentally in [25].

4. Bound states of several pulses and their stability

Below we will consider the formation of bound states of several pulses and investigate their stability in more detail. To this end, we will continue our analysis of the laser system with an active normal-dispersion fibre at a higher ($E_{\mathrm{sat\,slow}} = 30$ pJ) slow-component saturation energy. As simulation shows, this increase in the saturation energy increases the ratio of the dispersion-wave field energy to the pulse energy and, consequently, enhances the interaction of pulses through the general dispersion field and facilitates fast development of a particular scenario of their joint propagation.

In the first step we will consider initial conditions in the form of three 0.28-ps sech^2 pulses, located at different distances from each other. Propagation of these pulses is maintained at active-medium saturation energy $E_g > 120$ pJ; further results are obtained at $E_g = 130$ pJ. We modeled 10^4 cavity round trips.

The simulation results indicate that the initial distances between the pulses (10–20 ps) affect significantly the pulse-group evolution. If at least one of the initial distances is smaller than 12 ps, the bound state is not formed. A typical scenario is the attraction of pulses and their joint propagation with a random change in the interpulse distance. This regime can arbitrarily be referred to as a minibunch. It will be discussed in more detail below. Joint propagation of a bound state of two pulses and the third (individual) pulse is also observed.

A characteristic feature of pulse propagation is the formation of the aforementioned quasi-stationary states, in which there are an integer number of dispersion-wave periods between pulses. As in the case of two pulses, the drift under dispersion waves leads to a transition between quasi-stationary states and interaction of the stationary bound state of two pulses with the third pulse; under these conditions, an exchange between bound pulses or formation of a three-pulse bound state may occur [21].

Figures 6 and 7 show one of the ways to form a three-pulse bound state. As in the case of two pulses, it is reasonable to use the analogy with model pulses in a one-dimensional linear reservoir of dispersion waves. The drift velocity of a pulse is determined by the difference in the linear-wave intensities before and behind it. A bound state is formed when the average drift velocities of all pulses become equal; this equalisation occurs via interaction through long oscillating tails. If two pulses are bound through the general dispersion field (the distance between them is equal to an integer number of dispersion-waves periods), the influence of the third pulse can be considered as a small perturbation, leading to fluctuations of the interpulse distance. In this case, the perturbations leading the system to equilibrium (i.e., reducing the effect of lateral forces) become naturally advantageous. The process of changing the distances between pulses is shown in Fig. 7a. It can be seen that the perturbing effect of the third pulse causes only small fluctuations of the interpulse distance in each pair until this effect is resonantly summed with fluctuations of the dispersion field, which binds pulses in a pair. As a result, the interpulse distance changes stepwise; in each pair this distance changes by a dispersion-wave period. As a result, a stable bound state of three pulses with equal interpulse distances is formed (Fig. 7b). As simulations show, pulses fluctuate near the equilibrium position in this state, which corresponds to small interpulse-distance fluctuations.

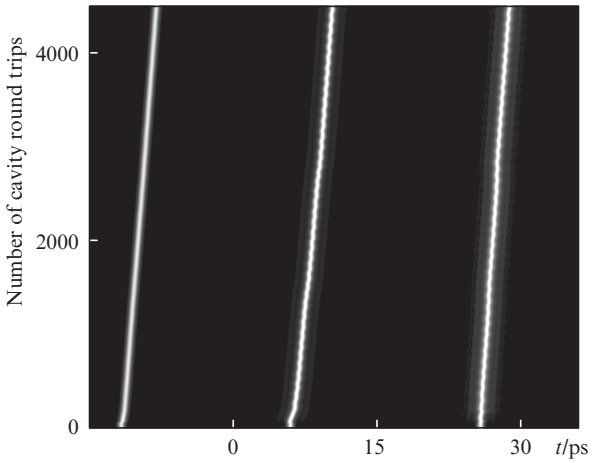

Figure 6. Trajectories of three pulses during the formation of a bound state.

Based on the above results, one can conclude that the interaction of a group of pulses through the general dispersion-wave field in the presence of a slow absorber component should lead to the formation of a bound state of pulses located at approximately equal distances from each other. However, this holds true for only a small number of pulses and a sufficiently large initial distance between them. In other cases one observes propagation of a noise group of closely located pulses, the distance between which randomly changes (a bunch). To clarify the origin of this bunch, we should consider the stability of bound states.

Figure 8 shows in a simplified form a deformation of a bound state, which is caused by fluctuation of the position of one of the pulses. The change in the slow-component absorption, corresponding to this fluctuation, is also shown. As was noted above, the change in the average pulse drift velocity is related to the change in the dispersion-wave intensity before and behind it and is caused by the difference in absorption because of the saturation of the slow absorber component.

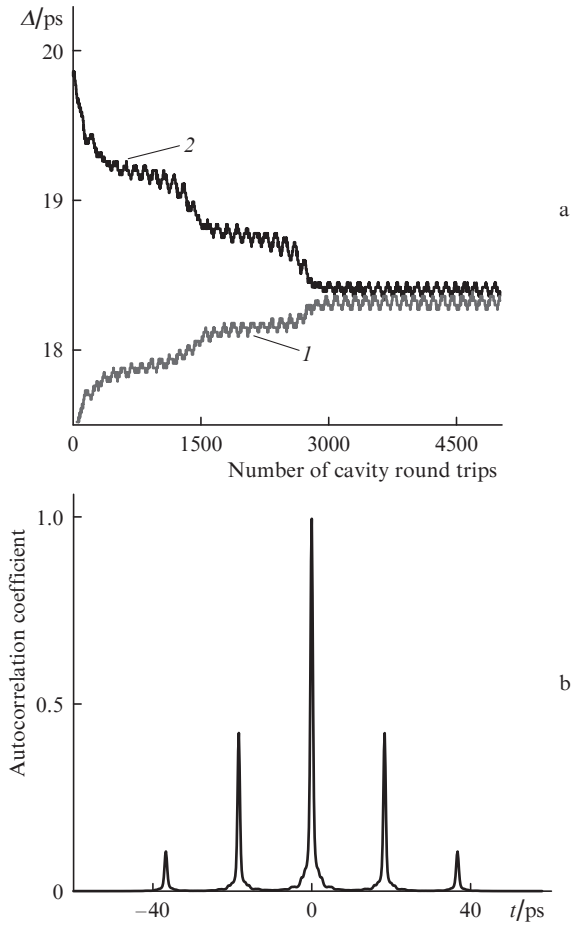

Figure 7. Formation of a bound state of three pulses. (a) The change in the interpulse distance [curves (*1*) and (*2*) show the distances between the first and second pulses and between the second and third pulses, respectively] and (b) the autocorrelation function of the bound state of three pulses, obtained by simulation.

This difference ($\Delta\alpha_{slow}$) is approximately described by expression (7).

It follows from (7) that the initial saturation of the slow component before the pulse, $\alpha_{slow}(t_p)$, is an important factor. When considering not very small saturation levels (i.e., an absorber with margin saturation), one can suggest that the bound-state deformation barely changes the $\alpha_{slow}(t_p)$ value and, therefore, the absorption difference $\Delta\alpha_{slow}$. Small fluctuations of the pulse position lead only to a small mismatch between the dispersion fields of pulses, which generate lateral forces, returning the pulse to the equilibrium position.

However, if the slow component is highly saturated (for example, because of the small distance between pulses or their large number in a group), the depth of the 'potential well' determining the pulse-position stability rapidly decreases. Under these conditions, a deformation of a bound state may induce an avalanche-like growth of instabilities and transformation of a regular bound state into a random bunch. Indeed, at a highly saturated slow component, even small fluctuations of the pulse position change significantly (decrease in Fig. 8) $\alpha_{slow}(t_p)$ and, therefore, reduce the absorption difference $\Delta\alpha_{slow}$ and the difference in dispersion-wave intensities. The latter effect leads to a decrease in the pulse drift velocity and, as a result, makes the first and second pulses come closer; their approach causes a further decrease in $\alpha_{slow}(t_p)$ and $\Delta\alpha_{slow}$ etc.

A small distance between pulses causes a wave of instabilities, which are related to deep saturation of the slow component of the absorber. A pulse located in an absorption minimum is maximally amplified, its duration decreases and the peak power and spectral width increase. Under these conditions, the limited width of the gain spectrum makes pulse splitting energetically favourable [1]. Thus, a low-absorption region (or several regions) arises, to which the energy of other pulses (which are at a disadvantage in competition for gain, being located in the region of high slow-component absorption) is transferred. As a result, one can observe a transformation of a group of pulses into a random bunch. This process in the system under consideration (at eight initial pulses) is shown in Fig. 9a.

Based on the above analysis, one can conclude that a bunch is formed at excessively deep saturation of the SESAM's slow component, which does not provide a stable

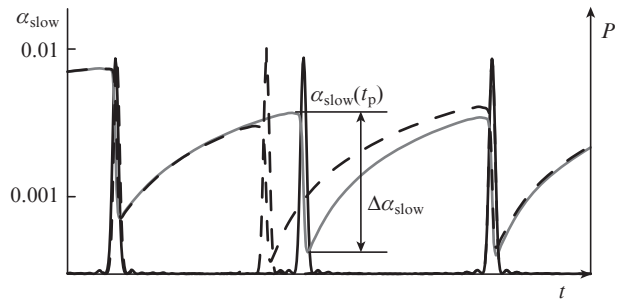

Figure 8. Schematic diagram of deformation of the bound state of several pulses: (solid lines) the initial states of pulses and the corresponding absorption coefficient of the SESAM's slow component and (dashed lines) the same dependence after a fluctuation of the interpulse distance.

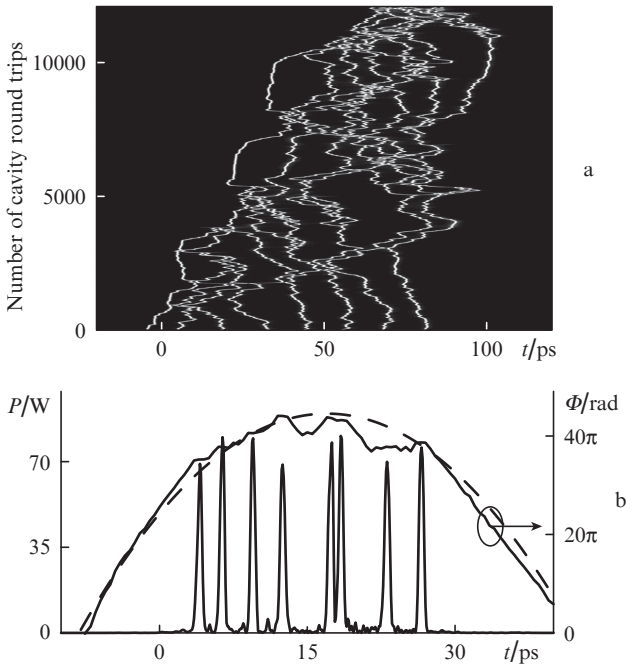

Figure 9. (a) Development of instabilities during propagation of an eight-pulse group and formation of a bunch of pulses and (b) pulse envelope and time dependence of the phase of an eight-pulse group after 12000 cavity round trips (the dashed line is a parabolic phase approximation: $\Phi - \Phi_0 = -c(t - t_0)^2/2$, $c = 4.4\times10^{23}$ s^{-2}).

position of an individual pulse. The simulation results show that the slow-component saturation energy $E_{\text{sat slow}}$, sufficient for maintaining the bound state stability, should constitute a significant part of the total pulse energy; its exact value is determined by the cavity parameters. In the case under consideration, a bunch is formed at $E_{\text{sat slow}} < 1/6$ of the total pulse energy; there may be no more than four pulses in the bound state. This condition is valid at only a sufficiently large initial distance between pulses (more than 40 pulse durations in our case).

Despite the strong interaction between pulses in a bunch, which now occurs not only via the dispersion-wave field but also through direct interpulse interactions, the joint pulse propagation is stable because of the attraction of pulses from the periphery to the bunch centre. This force originates from the Kerr nonlinear self-phase modulation by a group of pulses (Fig. 9b). Due to the nonlinearity of self-phase modulation, the rise in phase at the bunch edges can be approximated by a parabolic dependence $\Phi - \Phi_0 = -c(t - t_0)^2/2$, which, in turn, is indicative of approximately linear frequency modulation of a group of pulses with a modulation rate (chirp) c: $\Delta\omega \approx -c(t - t_0)$. In the case considered here, the nonlinear chirp of a group of pulses can be estimated as a rather large value ($c > 2.5\times10^{22}$ s^{-2}). One can see (Fig. 9a) that, when the extreme pulses are ejected beyond the bunch, an effective attractive force arises in the region of high-frequency modulation, because, when the cavity has intermediate anomalous dispersion, the group velocities at the leading and trailing edges are, respectively, lower and higher than the average bunch velocity [26, 27]. The above-described process makes the soliton bunch propagation stable.

The above simulation results are in agreement with experimental data. In particular, as experiments show, stationary bound soliton states with a symmetric autocorrelation function (i.e., constant interpulse distance) and a number of pulses as high as five or six can be generated. The interpulse distance amounts to several tens of individual soliton durations and depends on the cavity parameters: dispersion, gain spectrum width and SESAM characteristics. As was mentioned above, bound soliton states are generated only when the active fibre has normal dispersion. The increase in the number of pulses due to the increase in pumping or passive-fibre elongation (i.e., increased nonlinearity) leads to destruction of the bound state and formation of a bunch with closely located pulses. The interpulse distance in a bunch amounts to several soliton durations and constantly changes; nevertheless, the bunch propagates as a stable whole. The bunch width fluctuates; however, it is on average proportional to the number of pulses. The width fluctuations are caused by random displacements of pulses at the bunch boundaries [15, 18].

5. Conclusions

In this study we have analysed a soliton fibre laser with a semiconductor saturable absorber mirror; the latter is characterised by complex absorption relaxation dynamics, i.e., demonstrates both fast and slow relaxation. As experiments show, this laser exhibits interesting properties in the regime of multipulse generation. In particular, when the active medium has normal dispersion, pulses are mutually attracted to form stationary bound soliton states with an interpulse distance up to 100 pulse durations. Another version of group dynamics is the formation of a narrow bunch with a random change in the distance between pulses.

We have developed a laser model based on the description of pulse propagation in fibre elements using the Ginzburg–Landau equation and on the consideration of individual effects of lumped elements: saturable absorber, polariser and output coupler. The simulation has shown that the pulses generated by this laser system are characterised by a pulsating variation in parameters, which is related to partial transfer of pulse energy to the field of dispersion waves excited during amplification and transmission through discrete elements.

A simple fundamental model has been proposed to describe the interaction of pulses drifting under the action of linear dispersion waves. The slow component of saturable absorption determines the difference in the dispersion-wave intensities and the pulse drift velocity. The model developed explains the repulsion of pulses in the case of anomalous dispersion of the active fibre and their attraction under conditions of normal dispersion. The formation of the bound state of pulses is determined by the equalisation of drift velocities of pulses in their common dispersion field.

The stability of bound states is considered. It is found that it is mainly determined by the degree of saturation of the SESAM's slow component. This condition limits the pulse energy in the stationary bound state.

At a large number of pulses (or at a small distance between them), the slow component is in the highly saturated state, and the force induced by it from the side of dispersion waves with different intensities cannot prevent development of instabilities. In this case, a typical scenario involves the formation of a random pulse bunch, the width of which fluctuates around some average value, proportional to the number of pulses in the bunch. The bunch stability is caused by the manifestation of nonlinear self-phase modulation, which leads to frequency modulation of the group of pulses and their efficient attraction from the periphery to the bunch centre.

The results of numerical simulations are in fundamental agreement with experimental data. In continuation of this study, we are planning to consider in more detail the influence of the cavity parameters (dispersion, nonlinearity, gain, absorber saturation energy, etc.) on the characteristics of pulse groups and determine the critical values of the parameters corresponding to transitions between stationary bound states and random bunch.

Acknowledgements. This work was supported by the Ministry of Education and Science of the Russian Federation (State Order and Project No. 14.Z50.31.0015).

References

1. Kärtner F.X., der Au J.A., Keller U. *IEEE J. Sel. Top. Quantum Electron.*, **4**, 159 (1998).
2. Grudinin A., Gray S. *J. Opt. Soc. Am. B*, **14**, 144 (1997).
3. Kutz J.N., Collings B.C., Bergman K., Tsuda S., Cundiff S.T., Knox W.H., Holmes P., Weinstein M. *J. Opt. Soc. Am. B*, **14**, 2681 (1997).
4. Kutz J.N., Collings B.C., Bergman K., Knox W.H. *IEEE J. Quantum Electron.*, **34**, 1749 (1998).
5. Lederer M.J., Luther-Davis B., Tan H.H., Jagadish C., Akhmediev N., Soto-Crespo J.M. *J. Opt. Soc. Am. B*, **16**, 895 (1999).
6. Loh W.H., Grudinin A.B., Afanasjev V.V., Payne D.N. *Opt. Lett.*, **19**, 698 (1994).
7. Dianov E.M., Luchnikov A.V., Pilipetskii A.N., Starodumov A.N. *Opt. Lett.*, **15**, 314 (1990).

8. Dianov E.M., Luchnikov A.V., Pilipetskii A.N., Starodumov A.N. *Sov. Lightwave Commun.*, **1**, 37 (1991).
9. Pilipetskii A.N., Golovchenko E.A., Menyuk C.R. *Opt. Lett.*, **20**, 907 (1995).
10. Kivisto S., Hakulinen T., Kaskela A., Brown D.P., Nasibulin A.G., Kauppinen E.I., Harkonen A., Okhotnikov O.G. *Opt. Express*, **17**, 2358 (2009).
11. Okhotnikov O., Grudinin A., Pessa M. *New J. Phys.*, **6**, 177 (2004).
12. Okhotnikov O., Pessa M. *J. Phys. Condens. Matter*, **16**, S3107 (2004).
13. Suomalainen S., Guina M., Hakulinen T., Koskinen R., Paajaste J., Karialainen M., Marcinkevicius S., Okhotnikov O.G. *Mater. Sci. Eng. B*, **147**, 156 (2008).
14. Suomalainen S., Vainionpad A., Tengvall O., Hakulinen T., Karirinne S., Guina M., Okhotnikov O.G., Euser T.G., Vos W.L. *Appl. Phys. Lett.*, **87**, 121106 (2005).
15. Gumenyuk R., Okhotnikov O.G. *J. Opt. Soc. Am. B*, **29**, 1 (2012).
16. Okhotnikov O.G., Herda R. *Kvantovaya Elektron.*, **41**, 610 (2011) [*Quantum Electron.*, **41**, 610 (2011)].
17. Zhao L.M., Tang D.Y., Zhang H., Wu X. *Opt. Express*, **17**, 8104 (2009).
18. Gumenyuk R., Okhotnikov O.G. *J. Opt. Soc. Am. B*, **30**, 776 (2013).
19. Liu X. *Phys. Rev. A*, **84**, 053828 (2011).
20. Liu X.M., Wang L.R., Li X.H., Sun H.B., Lin A.X., Lu K.Q., Wang Y.S., Zhao W. *Opt. Express*, **17**, 8506 (2009).
21. Grelu P., Soto Crespo J.M. *Lecture Notes in Physics*, **751**, 137 (2008).
22. Akhmediev N., Soto-Crespo J.M., Grapinet M., Grelu Ph. *J. Nonlin. Opt. Phys. Mat.*, **14**, 159 (2005).
23. Soto-Crespo J., Akhmediev N., Grelu P., Belhache F. *Opt. Lett.*, **28**, 1757 (2003).
24. Akhmediev N.N., Ankiewicz A., Soto-Crespo J. *Phys. Rev. Lett.*, **79**, 4047 (1997).
25. Gumenyuk R., Okhotnikov O.G. *IEEE PTL*, **25**, 133 (2013).
26. Nguyen N.D., Binh L.N. *Opt. Commun.*, **282**, 2394 (2009).
27. Tamura K., Nakazawa M. *Opt. Lett.*, **21**, 1930 (1996).